TECHNICAL REPORT ARBRL-TR-02505

NUMERICAL MODELING OF ROTATING BAND FLOW FIELD AND COMPARISON WITH EXPERIMENT

James E. Danberg

July 1983

US ARMY ARMAMENT RESEARCH AND DEVELOPMENT COMMAND
BALLISTIC RESEARCH LABORATORY
ABERDEEN PROVING GROUND, MARYLAND

Destroy this report when it is no longer needed.
Do not return it to the originator.

Additional copies of this report may be obtained from the National Technical Information Service, U. S. Department of Commerce, Springfield, Virginia 22161.

The findings in this report are not to be construed as an official Department of the Army position, unless so designated by other authorized documents.

The use of trade names or manufacturers' names in this report does not constitute indorsement of any commercial product.

UNCLASSIFIED

SECURITY CLASSIFICATION OF THIS PAGE *(When Data Entered)*

REPORT DOCUMENTATION PAGE		READ INSTRUCTIONS BEFORE COMPLETING FORM
1. REPORT NUMBER TECHNICAL REPORT ARBRL-TR-02505	2. GOVT ACCESSION NO.	3. RECIPIENT'S CATALOG NUMBER
4. TITLE *(and Subtitle)* NUMERICAL MODELING OF ROTATING BAND FLOW FIELD AND COMPARISON WITH EXPERIMENT		5. TYPE OF REPORT & PERIOD COVERED Final 6. PERFORMING ORG. REPORT NUMBER
7. AUTHOR(s) James E. Danberg		8. CONTRACT OR GRANT NUMBER(s)
9. PERFORMING ORGANIZATION NAME AND ADDRESS U.S. Army Ballistic Research Laboratory ATTN: DRDAR-BLL Aberdeen Proving Ground, Maryland 21005		10. PROGRAM ELEMENT, PROJECT, TASK AREA & WORK UNIT NUMBERS RDT&E 1L162618AH80
11. CONTROLLING OFFICE NAME AND ADDRESS US Army Armament Research & Development Command US Army Ballistic Research Laboratory (DRDAR-BLA-S) Aberdeen Proving Ground, MD 21005		12. REPORT DATE July 1983 13. NUMBER OF PAGES 40
14. MONITORING AGENCY NAME & ADDRESS*(if different from Controlling Office)*		15. SECURITY CLASS. *(of this report)* Unclassified 15a. DECLASSIFICATION/DOWNGRADING SCHEDULE

16. DISTRIBUTION STATEMENT *(of this Report)*

Approved for public release, distribution unlimited.

17. DISTRIBUTION STATEMENT *(of the abstract entered in Block 20, if different from Report)*

18. SUPPLEMENTARY NOTES

19. KEY WORDS *(Continue on reverse side if necessary and identify by block number)*

Projectile Rotating Band
Turbulent Boundary Layer
Supersonic Drag
Parabolized Navier-Stokes Code

20. ABSTRACT *(Continue on reverse side if necessary and identify by block number)*

A numerical model for supersonic, turbulent flow over a projectile rotating band is described. An approximate geometric representation for the separation regions ahead of and behind the band is used to create realistic compression and expansion regions in the projectile boundary layer. The upstream and downstream ramp are found roughly consistant with the expected interaction regions as observed on forward and backward facing steps.

The c lculated maximum and minimum pressures agree well with data obtain-

DD FORM 1 JAN 73 1473 EDITION OF 1 NOV 65 IS OBSOLETE

UNCLASSIFIED

SECURITY CLASSIFICATION OF THIS PAGE *(When Data Entered)*

20. ABSTRACT (Continued)

ed on a 6 caliber Secant-Ogive-Cylinder model tested in the Naval Surface Weapons Center supersonic wind tunnel at Mach number of 3. Boundary layer profiles were measured on, and downstream of the rotating band using a Laser Doppler Velocimeter. These profiles were not adequately predicted by the theory suggesting that the turbulence model used did not respond to the rapidly changing flow conditions in a physically realistic way.

TABLE OF CONTENTS

LIST OF ILLUSTRATIONS

I. INTRODUCTION

The accuracy and range of small arms and artillery have been significantly improved by the use of rifled gun barrels. Rifling causes the projectile to spin rapidly during launch. To insure that slip between the rifling and shell is eliminated, rotating bands were added to projectiles and are now a standard component. These bands are made of soft metal and are slightly larger than the bore. Although the band is desirable in producing spin while the projectile is in the gun tube, it is undesirable after launch because the added cross-sectional area and irregular shape produces added aerodynamic drag. A 5% increase in drag is a nominal estimate for an artillery shell and increases for small caliber bullets because of the relatively large rotating bands required. There is also evidence that the band affects the pitching and magnus moments of the shell.

The objective of the present investigation is to incorporate a numerical model of the geometry of a rotating band into existing computer programs designed to predict the aerodynamic characteristics of the projectile. The Ballistic Research Laboratory has had considerable success in using parabolized Navier-Stokes codes in predicting effects of ogive-cylinder-boattail geometries on drag, normal force and moments. Modifications to include effects of surface irregularities would make the numerical simulations more realistic and complete.

This report summarizes the results of some recent investigations aimed at developing a rotating band model for use with the BRL codes. First, a brief review of existing experimental data on rotating band drag sets the work into perspective. The second section is concerned with the development of the rotating band model geometry which has been incorporated into the PNS code. Finally, a comparison is made between the numerical results and the data from a Naval Surface Weapons Center experiment.

II. BACKGROUND

A currently recommended procedure for estimating rotating band drag has been incorporated into the computer code "McDrag"[1] developed by R. McCoy of BRL. The additional band drag coefficient is estimated in that code as shown by the solid line in Figure 1 where $C_{D_{RB}}/(d_{RB} - 1)$ is plotted against Mach number. This curve was originally suggested by F. Moore[2] and is based on a

---

1. *McCoy, R.L., "'MCDRAG' - A computer Program for Estimating the Drag Coefficients of Projectiles," ARBRL-TR-02293, U.S. Army Ballistic Research Laboratory, ARRADCOM, February 1981 (AD A098110).*

2. *Moore, F.G., "Body Alone Aerodynamics of Guided and Unguided Projectiles at Subsonic, Transonic and Supersonic Mach Numbers," NWL Technical Report TR-2796, November 1972.*

series of wind tunnel tests[3] he performed using the basic Naval 5"/38 RAP projectile of about 4 calibers total length. Although there is considerable scatter in the data, the line reasonably well represents the results except perhaps in the low transonic region.

Moore's experiment involved only one basic model size and one size rotating band. He recommended presenting the results in this form presumably because he anticipated the added drag of the band was pressure drag which would vary directly in proportion to the projected frontal area of the protuberance.

There is relatively little corroborating data available. Charters[4] in a 1947 paper discusses "banding" of a 20mm projectile. The results cited are generally consistent with Moore's data but the paper lacks specific dimensions for a more quantitative comparison.

In a later series of experiments, Scott[5] obtained free-flight data on the Army-Navy Spinner Rocket at Mach number 1.8 with several band configurations. Some of Scott's observations agree with Moore's data but they also show that the drag of the band was configuration dependent. Figure 1 shows a number of Scott's data points representing several different configurations. The highest point represents the largest band size (d_{RB} = 1.04) positioned 3.4 calibers from the nose. The lowest data point is a smaller band (d_{RB} = 1.02) in the same position. This latter case represents the rotating band of a 105mm projectile scaled to that of a 20mm model. The intermediate point is a d_{RB} = 1.02 band located 5.4 calibers or 2 calibers farther aft. The variation of drag coefficient with position remains unexplained.

A comprehensive review of aircraft two-dimensional excrescence drag has been published in 1981 by Young and Patterson[6] as AGARDograph 264. This review covers discrete and distributed roughness elements and describes their contribution to aircraft drag. Although a great many research and applied experimental studies were considered, nothing is mentioned regarding the effects of protuburances on projectiles. All the experimental data considered, particularly as regards small rectangular steps, are correlated in terms of C_D / C_f as a function of free-stream Mach number and $h^+ = u_\tau h/\nu$. When their

---

3. *Moore, F.G., "A Study to Optimize the Aeroballistic Design of Naval Projectiles," NWL TR-2337, September 1969.*

4. *Charters, A.C., "Some Ballistic Contributions to Aerodynamics," Journal of Aeronautical Science, Vol. 14, No. 3, 1947, pp. 155-166.*

5. *Scott, W.E., "The Effect of Rotating Band Upon Some Aerodynamic Coefficients of the Seven Caliber Army-Navy Spinner Rocket at Mach 1.8," BRL-MR-1302, U.S. Army Ballistic Research Laboratory, ARRADCOM, September 1960 (AD 246223).*

6. *Young, A.D., and Patterson, J.H., "Aircraft Excrescence Drag," AGARDograph No. 264, July 1981.*

recommended drag calculation is performed for the condition of Moore's experiment, the drag coefficient is a factor of 2.5 times higher than that recommended by Moore, although the trend with Mach number is in reasonable agreement.

The conclusions to be drawn from this brief review of rotating band measurements are:

1. The added drag of the band is small on the order of 5% of the total drag and is a maximum in the transonic speed range.

2. The correlations of the experimental data are not sufficient to accurately define the drag within a factor of two. This is probably because in wind tunnel and ballistic range experiments it is necessary to take the difference between the relatively large drag with and without the band to find the much smaller band drag.

3. Pressure distribution measurements in the vicinity of the band might be a more sensitive method of extracting the force acting on the band.

4. If the correct perturbation of the viscid and inviscid flow field can be obtained in computer models, they may be expected to predict the effects of the rotating band on downstream skin friction, separation and base pressure effects.

III. COMPUTER MODEL OF ROTATING BAND

Ideally it would be desirable to specify the geometry of the rotating band and apply a full Navier-Stokes solver to the compressible and viscous surrounding flow. However, solutions of the Navier-Stokes equations for flows including regions of locally separated flow are not yet routine. It would require a major effort to produce such solutions. As an intermediate step to the development of a rigorous technique, a relatively simple modification to the steady-state, space marching parabolized Navier-Stokes (PNS) code has been constructed. The code is based on the work of Sturek and Schiff.[7]

A. Assumed Features of the Rotating Band Flow Field

The flow field in the vicinity of the rotating band is assumed as indicated in Figure 2. The band is assumed to be smaller than the local boundary layer thickness and that the effect of the band is to induce embedded regions of separated flow ahead of and behind the protuburance. The turning of the flow by the separated regions produces weak compression waves which propagate into the inviscid flow and may coalesce into shock waves. The flow reattaches on top of the band where it turns approximately parallel to the band. At the trailing edge, the flow again turns to follow the separated flow region and

---

7. *Sturek, W.B., and Schiff, L.B., "Numerical Simulation of Steady Supersonic Flow Over Spinning Bodies of Revolution," AIAA Journal, Vol. 20, No. 12, December 1982, pp 1724-1731.*

the main flow reattaches to the projectile some distance downstream. Compression waves produce the gradual turning of the flow so that after reattachment the boundary layer grows in a constant pressure region.

These are the primary elements in the physical flow model. Note that the pressure rise associated with the compression waves actually precedes the separation point of the boundary layer flow. The extent of the upstream pressure rise can be estimated by considering the results of experiments on forward and backward facing steps. Figure 3 shows typical pressure distribution observations for these two situations. This figure is from the work of Chapman, et al[8] as reported by Chang.[9] The forward facing step with turbulent boundary layer shows that the pressure begins to rise ahead of the separation point, s, and reaches 2.2 times the ambient value for this particular configuration. On the other hand, the backward step shows a sharp 65% pressure drop from the ambient value just behind the step with a more gradual return downstream. These results confirm in general the physical situation assumed in Figure 2.

Separation length data from a number of sources is summarized in Figure 4 and 5 again taken from Chang.[9] Although these figures show some dependency of the separation length on Reynolds number, Mach number and geometry, the magnitude for the high Reynolds number turbulent flow of between 5 and 6 is remarkably the same for both forward and backward facing steps. From these observations it may be concluded that the total interaction length is of the order of 10 step heights before and behind the band.

B. PNS Code Model Rotating Band

After considering the previous data the geometry of the projectile in the vicinity of the band was specified as shown in Figure 6. Given the height of an actual band, the upstream and downstream interaction regions are specified by an interaction length, L, and a functional form for a surface which produces the same pressure rise as the actual flow field. This surface may be considered as roughly a dividing streamline separating the separated flow region from the rest of the boundary layer. This is not literally correct because the function extends beyond the separated region to produce the upstream and downstream pressure effects. It is not a true dividing streamline because the no-slip boundary condition is applied to this surface whereas the dividing streamline does have a slip velocity due to viscous effects.

The functional form was chosen arbitrarily as:

---

8. *Chapman, D.R., Kuehn, D.M., and Larson, H.K., "Investigation of Separated Flows in Supersonic and Subsonic Streams with Emphasis on the Effect of Transition," NACA TN 3869, 1957.*

9. *Charwat, A.F., Roos, J.N., Dewey, C.F., and Hitz, J.A., "An Investigation of Separated Flows: Part I - The Pressure Field," Journal of the Aerospace Sciences, Vol. 28, No. 6, June 1961, pp. 457-470.*

$$r_b = r + h\, f\,(x/L) \qquad (1)$$

where

$$f\,(x/L) = \begin{cases} 1 - \cos\left(\frac{\pi}{2}\,\frac{x}{L}\right) \\ \\ (x/L)^{n+1} \end{cases} .$$

Note that both functions have their maximum slope at x = L. If small perturbation arguments are used, the maximum pressure on the upstream ramp corresponds to the maximum slope. The maximum pressure rise can be increased by decreasing L. In using the cosine function the minimum L that can be used is apparently limited by local separation on the ramp. In order to eliminate the separation various functional forms were tried in an attempt to tailor the slope distribution and thereby the adverse pressure gradient so as to prevent separation. The power law shape has a slower rate of increase in slope than the cosine shape followed by a more rapid increase near the band. Higher maximum slopes can be achieved with the power law shapes and thus higher maximum pressures.

The ramp characteristic length, L, is assumed to represent the interaction length and based on the previous discussion it is expected to be on the order of 10 band heights. The lengths used were varied in the computations so as to obtain agreement between the calculated pressure distribution and some measurements obtained at the Naval Surface Weapons Center.

IV. COMPARISON WITH EXPERIMENT

The Ballistic Research Laboratory sponsored a series of wind tunnel tests at the Naval Surface Weapons Center, White Oak Laboratory, on a projectile model with and without a rotating band. Complete details of the experiment will be published as a NSWC Technical Report.[10] The following brief discussion of the experiment is limited to only those aspects pertinent to the present comparison with the PNS results.

A. BRL-NSWC Experiment

The BRL Secant-Ogive-Cylinder (SOC) model (57.15mm in diameter) was modified by attaching two rotating band configurations for these tests. The general configuration of the model is given in Figure 7 along with the conditions of the test.

The primary measurements included the model pressure distribution and boundary layer characteristics. The NSWC laser velocimeter was used to obtain mean velocity and turbulence profiles through the boundary layer at four

---

10. Yanta, W. and Gorney, J., NSWC/WOL unpublished wind tunnel data, private communication.

stations, one ahead, one on top and two downstream of the band.

The tests were made at a Mach number of 3.02 and with atmospheric supply conditions which results in a Reynolds number based on model diameter of 5.5×10^6.

Figure 8 is a Schlieren photograph from these tests which shows the compression waves originating from in front of and behind the rotating band. Waves are also generated by the trip mechanism located near the nose. The transition trip insured a fully turbulent boundary layer over the rotating band.

B. Comparison Between PNS Code and Experiment

Figure 9 shows the comparison between the pressure distribution predicted by the PNS code and the NSWC measurements. The center of the band is located at 4.39 calibers from the nose and the band is 2mm high (h/D = .0356) and 12.7mm wide. The measured pressures are given in Table 1 which also defines the location of the pressure taps.

TABLE 1. PRESSURE DISTRIBUTION DATA ROTATING BAND SOC MODEL

h/D =	0.0 (1)	0.0178	0.0356
X/D	$p_w/\gamma p_\infty$	$p_w/\gamma p_\infty$	$p_w/\gamma p_\infty$
0.889	1.200	1.245	1.238
1.556	1.044	1.074	1.061
2.222	0.918	0.927	0.932
2.791	0.819	(2)	(2)
3.129	0.577	0.586	0.592
3.222		0.559	0.572
3.556	0.582	0.571	0.579
4.222	0.618	1.144	1.559
4.556		0.330	0.224
4.889	0.636	0.602	0.582
5.333	0.640	0.632	0.656
5.611	0.652	0.650	0.680
5.778		0.645	0.656
BASE		1.368	0.758

p_0 = 1.238 atm.
T_0 = 322 K
M_∞ = 3.02

NOTE: (1) Reklis and Sturek, Ref. 11.
(2) Bad Data point.

11. *Reklis, R.P., and Sturek, W.B., "Surface Pressure Measurements on Slender Bodies at Angle of Attack in Supersonic Flow," ARBRL-MR-02876, U. S. Army Ballistic Research Laboratory, ARRADCOM, Aberdeen Proving Ground, MD 21005, November 1978 (AD A064097).*

Excellent agreement is obtained between the PNS computation and the measured pressures in all regions unaffected by the band which generally confirms the quality of the method. Only two points are substantially affected by the presence of the protuberance; these taps are located 3mm ahead of and behind the band. The predicted pressures in this area agree relatively well with these two measurements. Between the maximum and minimum values the pressure drops very rapidly, undershoots and then trys to stabilize near the undisturbed level. It is not clear whether this rather large oscillation is related to the numerical procedure when subject to such a rapid change in conditions or whether the flow actually over expands when reattaching on the model. More detailed pressure measurements are required in that region to answer this question. The shape of the band in these computations was the power law equation with n = 1, and with L = 7.5h. The relaxation of the pressure to the undisturbed level behind the band is also well predicted by the PNS code.

Similar results were obtained for the smaller band case (h = 1mm) as shown in Figure 10. The cosine function was used in this case but the interaction length was L = 10h. The high and low peaks may be under predicted here because the pressure taps are still located ±3mm from the band which is now ±3 step heights. Thus, the measured pressures may be somewhat less than the actual peak pressures.

C. Boundary Layer Profiles

As has already been pointed out, boundary layer velocity profiles were obtained at four stations as part of the experiment. The measurements were made using a two-component laser doppler velocimeter. This equipment permitted the measurement of mean u velocity parallel to the model axis and the mean v component normal to the surface. Turbulent fluctuating quantities such as $\sqrt{\overline{u'^2}}$, $\sqrt{\overline{v'^2}}$ and the Reynolds stress $\overline{u'v'}$ were also obtained. Prediction of the turbulence characteristics based on the PNS algebraic turbulence model are being developed but will not be considered here.

The mean u component of the velocities are shown in Figure 11 for the 2mm band and in Figure 12 for the 1mm band. In both sets the first Figures 11a and 12a represent the boundary layer approaching the band. This station is 0.28 calibers ahead of the band or 7.8 step heights for the large band and 15.8 step heights for the smaller band case. These upstream profiles are well predicted by the PNS code which is consistent with the quality of the codes results for all smooth projectile configurations. The profiles on top of the band (Figure 11b and 12b) are significantly different from the prediction, both in shape and magnitude. Near the outer edge of the calculated profile is a local low speed region which corresponds to the compression waves generated by the upstream ramp. No sign of this is observed in the experimental data, but the range of the data in distance normal to the wall is rather limited. Close to the wall the velocity is considerably less than the prediction. Some possible reasons for the discrepancies are:

1. Numerical: i.e., the change in conditions is too rapid for the grid distribution used.

2. Geometrical: i.e., the band geometry is arbitrary chosen and may be incorrect.

3. The turbulence model employed is unable to respond correctly to the rapid expansion at the top of the band.

4. Experimental: i.e., the laser velocimeter results depend on tracer particles in the flow following the fluid motion; with rapidly changing conditions the particles may not respond fast enough.

Downstream of the band the profiles slowly relax toward the undisturbed boundary layer. Figures 11c,d and 12c,d show this development. The small band produces a smaller perturbation and its effects die out faster. The X/D = 4.70 and 5.75 stations are 0.20 and 0.75 model diameters, respectively, behind the rotating band which means that they are 5.6 and 21 step height downstream. Using the upstream station to evaluate the boundary layer thickness, these stations are approximately 3 and 11 boundary layer thicknesses downstream. Based on these results it appears that on the order of 15-20 boundary layer thicknesses would be required for the boundary layer to return to the undisturbed state. The numerical theory relaxes in a much shorter distance.

D. Skin Friction Coefficient

Figures 13 and 14 show the calculated skin friction coefficient distribution and its rather major fluctuation in the vicinity of the rotating band. These calculations show that the more severe adverse pressure gradient upstream of the large rotating band brings the flow to the verge of separation, i.e., $c_f = 0$. It is this condition that limits the maximum pressure rise which can be developed with the model band. Because the model band does not correctly represent the separated flow ahead of and behind the band, it is not correct to integrate this friction distribution to determine the skin friction contribution to the rotating band drag. Nevertheless, it may be anticipated that the c_f contribution to band drag will be small because of: (a) the small areas affected by the perturbations and (b) the rough balance between the regions of decreased friction (adverse pressure gradient regions) and the increased friction on the top of the band.

E. Pressure Drag Coefficient

Normally, integration of the axial component of the model band pressure distribution over the area of the band could be used to give the drag acting on the model band. It is not clear that such a procedure would correctly estimate the actual band drag because it is the local pressure acting on the forward and rearward face of the band which contributes to the physical band drag. With this assumption it is possible to use the measured pressure data or the maximum and minimum theoretical pressures to estimate the rotating band C_D. The relationship between the pressures and C_D is

$$\frac{C_{D_{RB}}}{d_{RB} - 1} = \left(\frac{p_{max}}{\gamma\, p_\infty} - \frac{p_{min}}{\gamma\, p_\infty}\right) \frac{4}{M_\infty^2}\,, \qquad (2)$$

which for the data in Table 1 gives

$$\frac{C_{D_{RB}}}{d_{RB} - 1} = \begin{cases} 0.60 \ ; \ h/D = 0.0356 \\ \\ 0.36 \ ; \ h/D = 0.0178. \end{cases} \tag{3}$$

The small band drag agrees with the Moore correlation whereas the large band is in better agreement with Young and Patterson as can be seen by referring to Figure 1. This indicates that the drag coefficient is a function of the size of the band as well as the Mach number.

V. CONCLUDING REMARKS

It has been the objective of this report to describe a numerical model for the flow over a rotating band and to compare the results of this model with experimental data obtained at the NSWC on the BRL Secant-Ogive-Cylinder Model.

The results of this investigation shows that the maximum and minimum pressure can be predicted using a parabolized Navier-Stokes computational technique employing an approximate, but realistic, geometric model of the flow in the vicinity of the band. The separation regions ahead of and behind the band are approximated by compression ramps with expansion corners at the forward and rear edges of the rotating band. By suitable choices of the form of the ramps the boundary layer flow is decelerated without producing local separation. The upstream and downstream extent of the ramp is roughly consistent with the interaction distance measured on forward and backward facing steps.

The details of the velocity boundary layer near the band are not correctly predicted by this theory. Further investigation of the turbulence model employed and additional experimental data are required to help explain this discrepancy. Calculations of parasitic projectile drag based on maximum and minimum pressures associated with the rotating band are dependent on size of the band and not just Mach number as suggested by the methods currently in use. Skin friction drag is found to contribute very little to the overall drag although no estimate of the effect of the perturbation in the boundary layer on the base drag has been or can be made using the present PNS code. The numerical results indicate that the disturbance caused by the band dies out in a few boundary layer thicknesses (much faster than observed experimentally) and therefore little downstream influence is predicted.

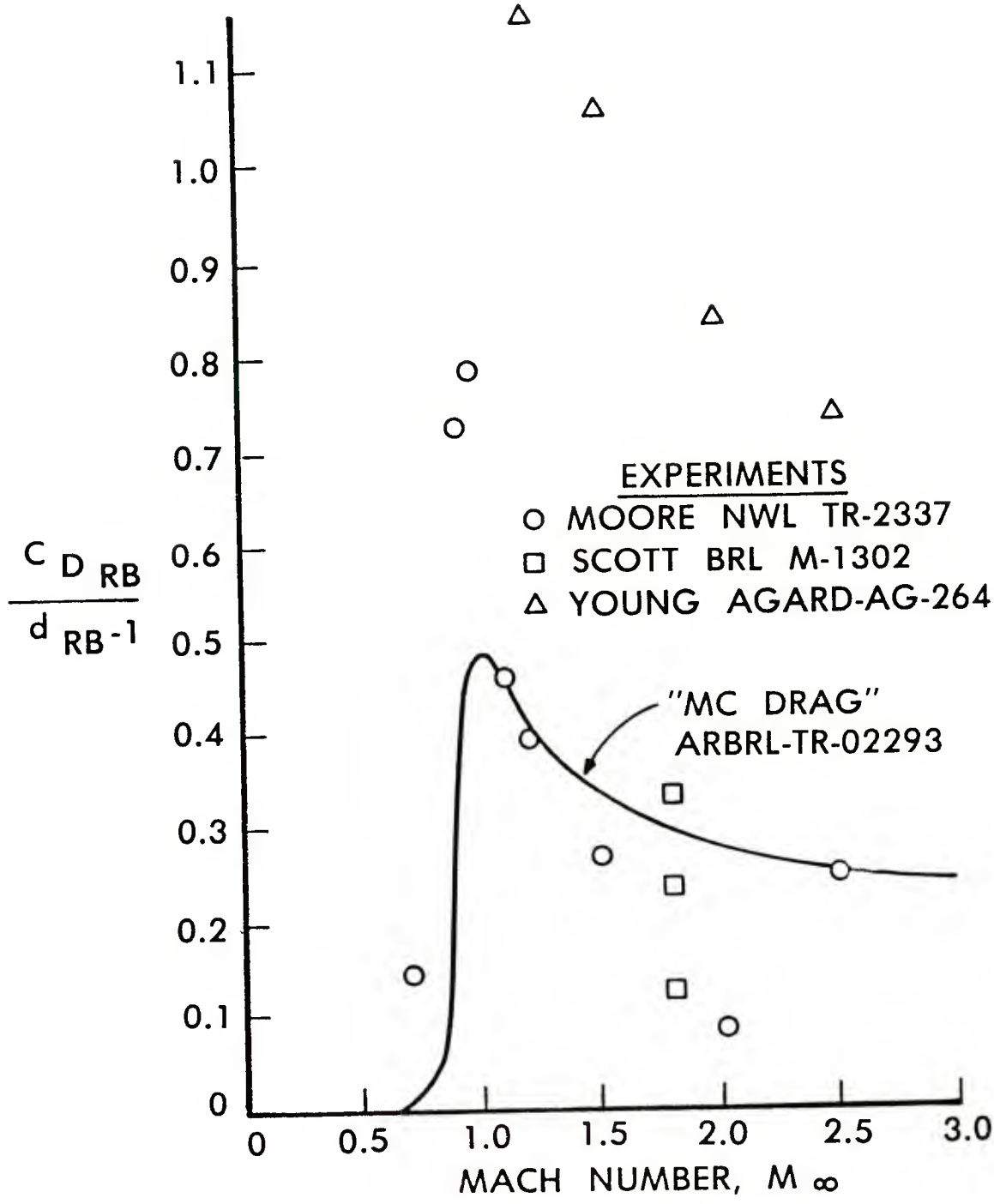

Figure 1. Rotating Band Drag Coefficient

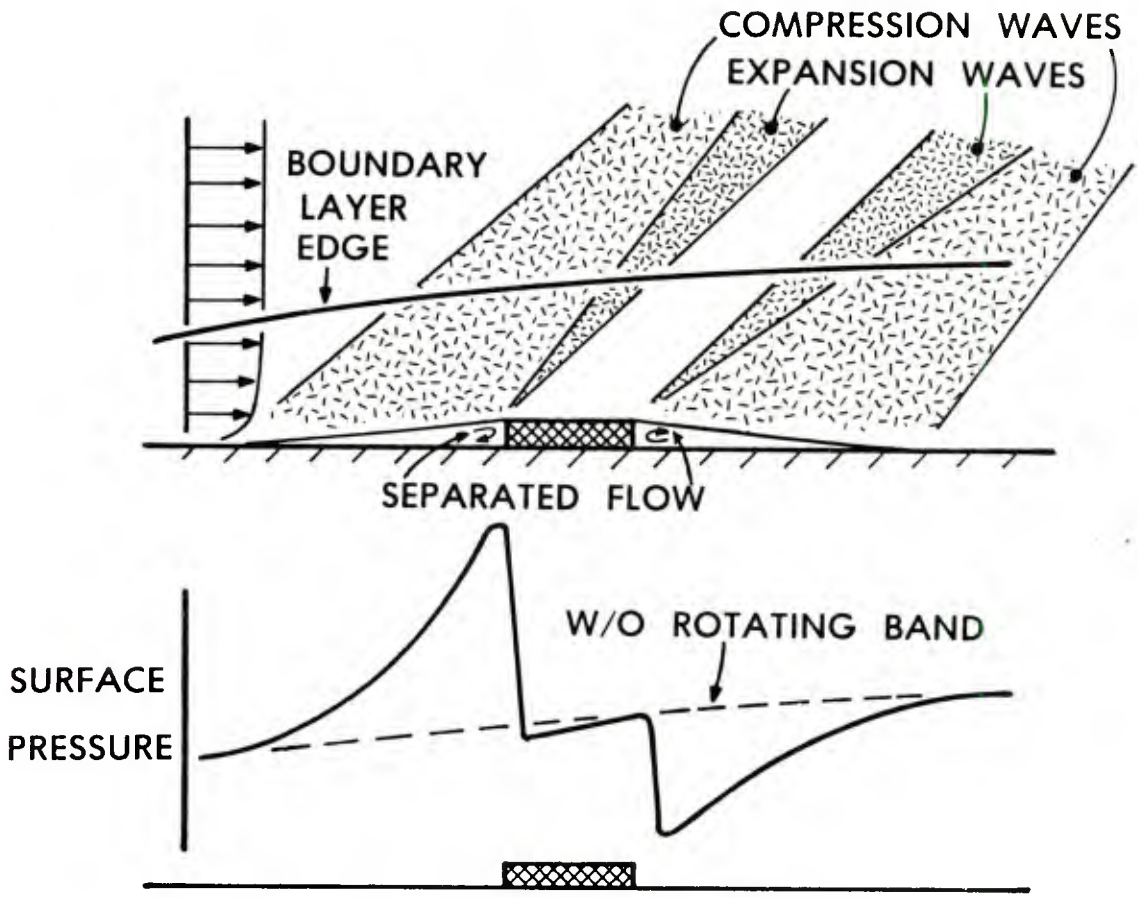

Figure 2. Rotating Band Flow Field

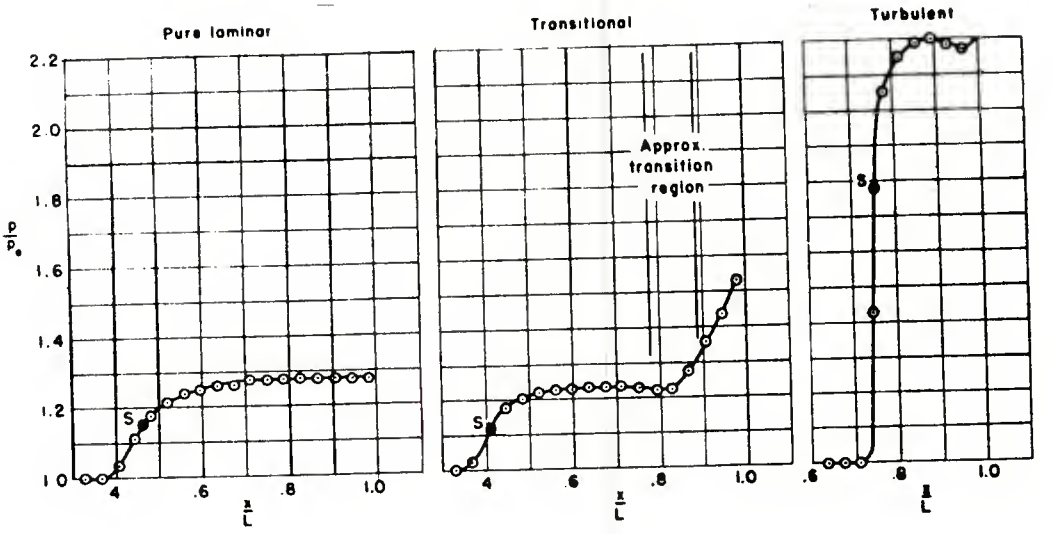

(a) Forward Facing Step

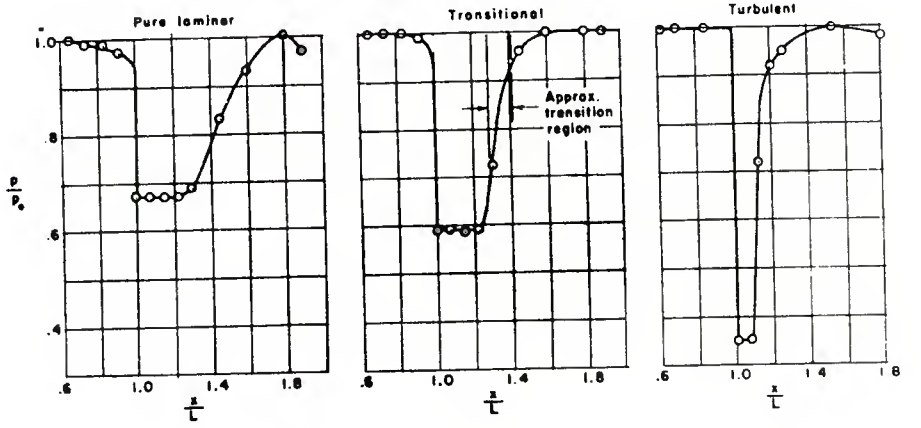

(b) Backward Facing Step

Figure 3. Typical Pressure Distributions for Forward and Backward Facing Steps

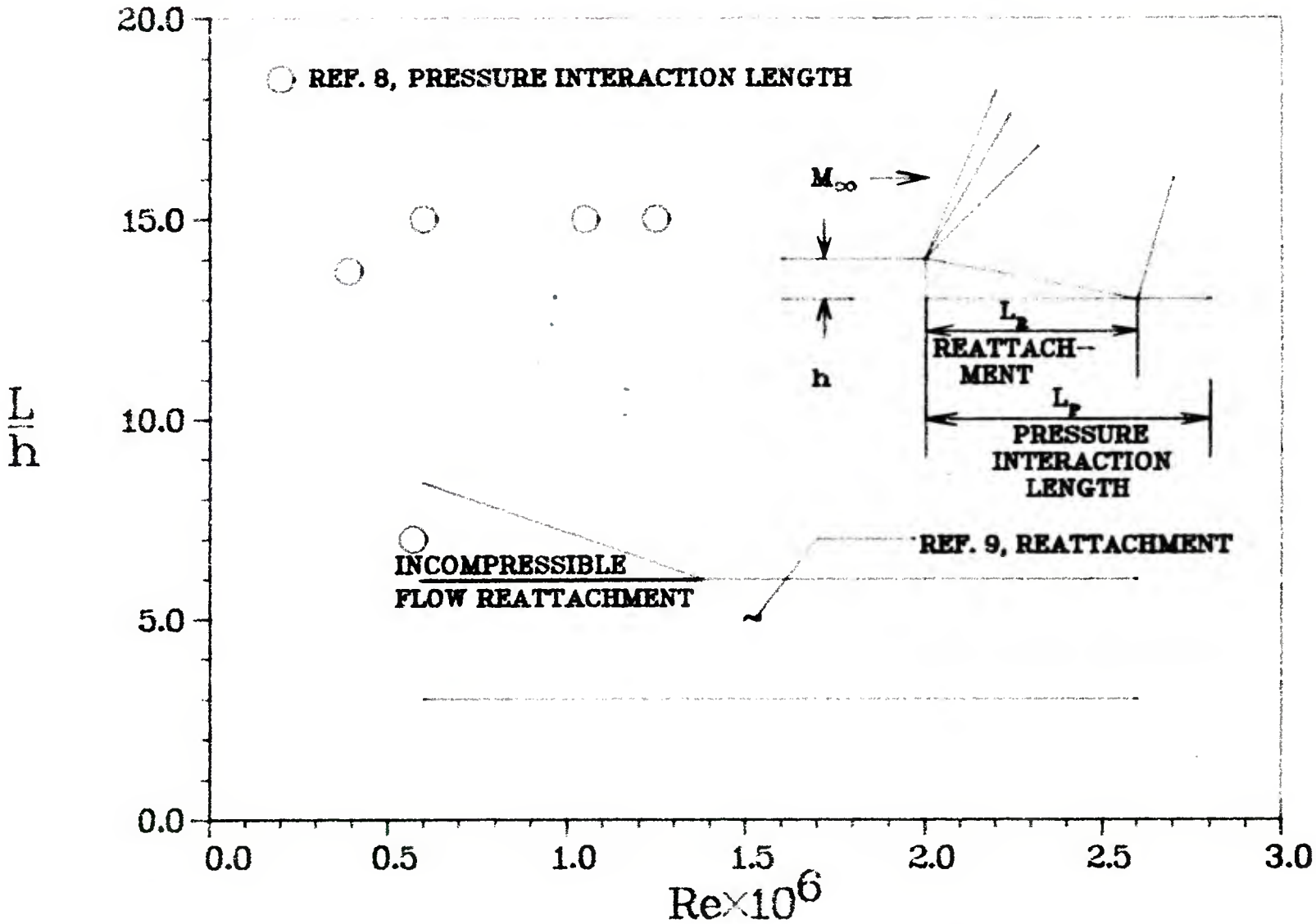

Figure 4. Reattachment and Pressure Interaction Length for Backward Facing Step

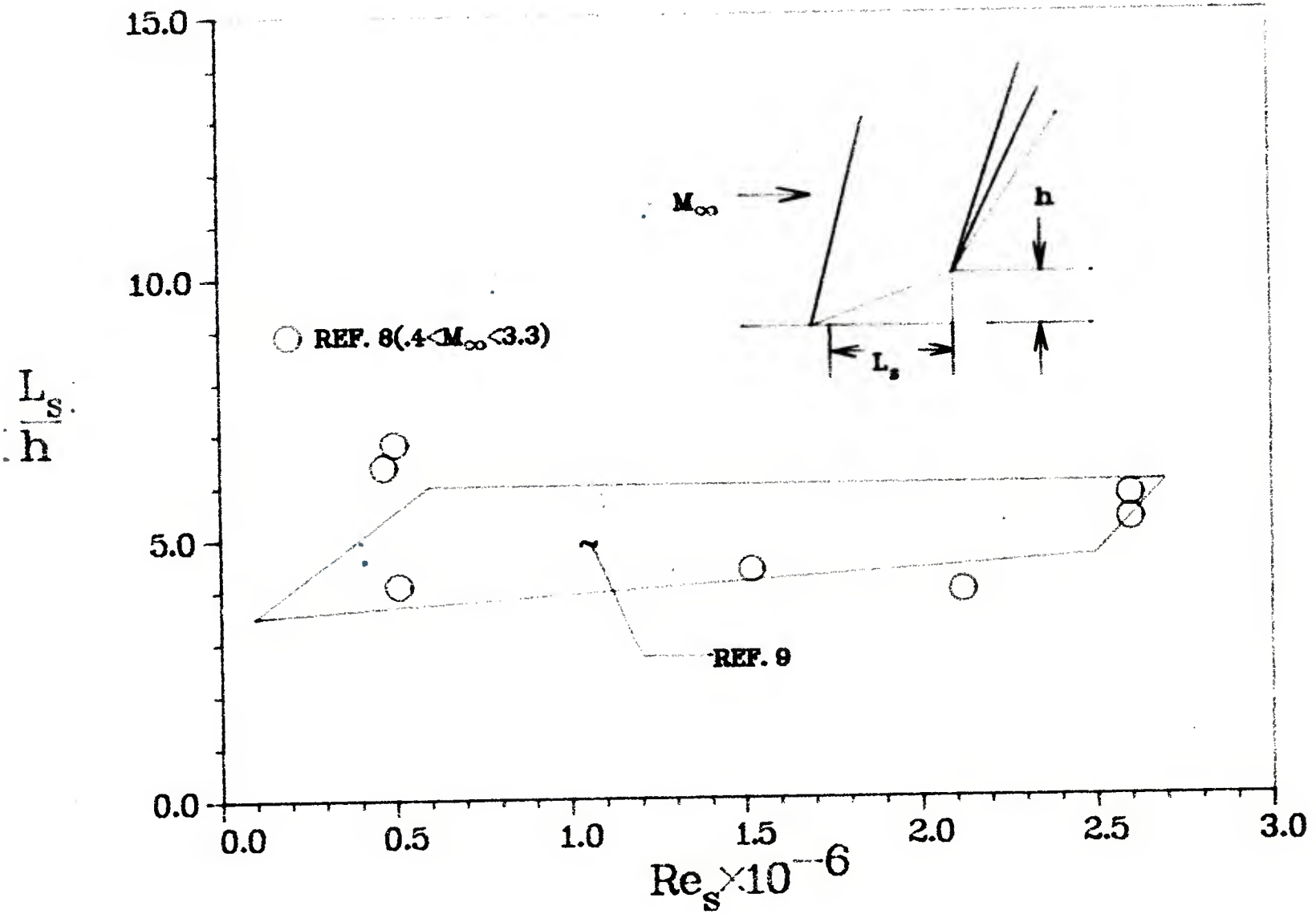

Figure 5. Separation Length for Turbulent Flow Over a Forward Facing Step

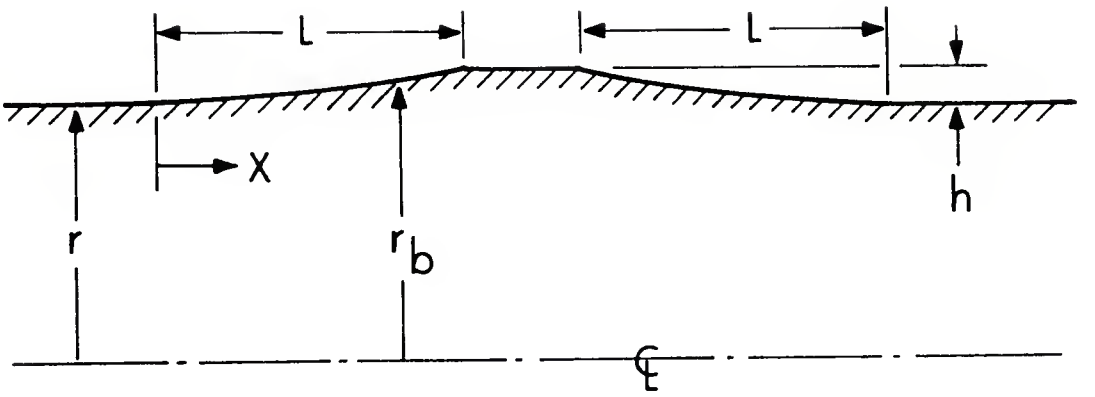

$$r_b = r + h\ f_n\ (X/L)$$

$$f_n(X/L) = \begin{cases} (X/L)^2 \\ 1 - \cos\left(\frac{\pi}{2}\ \frac{X}{L}\right) \end{cases}$$

NEGLECTS SLIP BOUNDARY CONDITION ON DIVIDING STREAMLINE

Figure 6. PNS Rotating Band Model

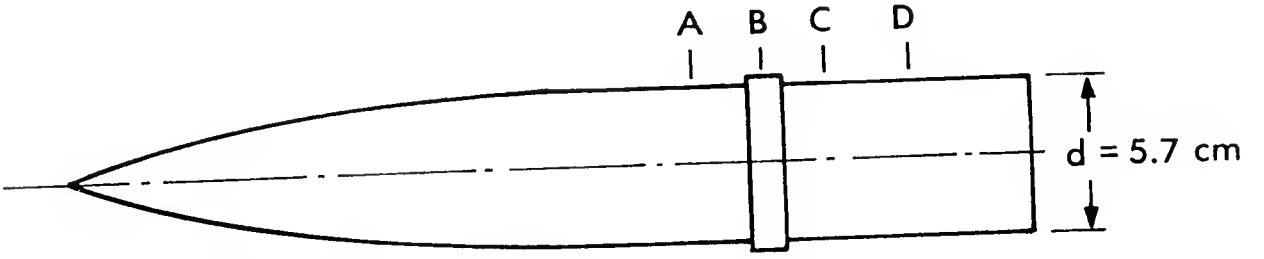

TEST CONDITIONS

M = 3

$\alpha = 0^{\circ}, 2^{\circ}$

$Re = 5.5 \times 10^{6}$

ROTATING BAND HEIGHT

h = 0.0178 AND 0.0356 cal

MEASUREMENTS

LDV STATIONS A 4.00 cal
B 4.39 cal
C 4.70 cal
D 5.25 cal

WALL PRESSURE DISTRIBUTION

SPARK SHADOWGRAPHS

Figure 7. BRL-NSWC/WOL Experimental SOC Model

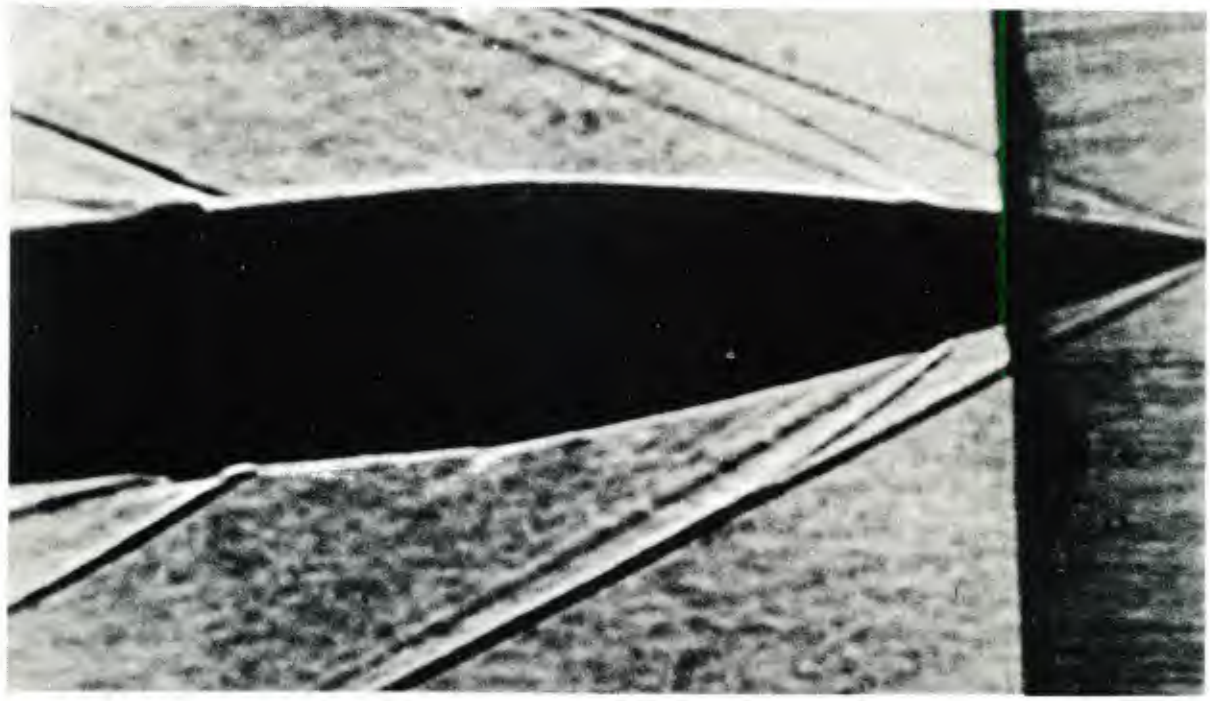

Figure 8. Shadowgraph of SOC Model with Rotating Band in NSWC/WOL Wind Tunnel, $M_\infty = 3.0$

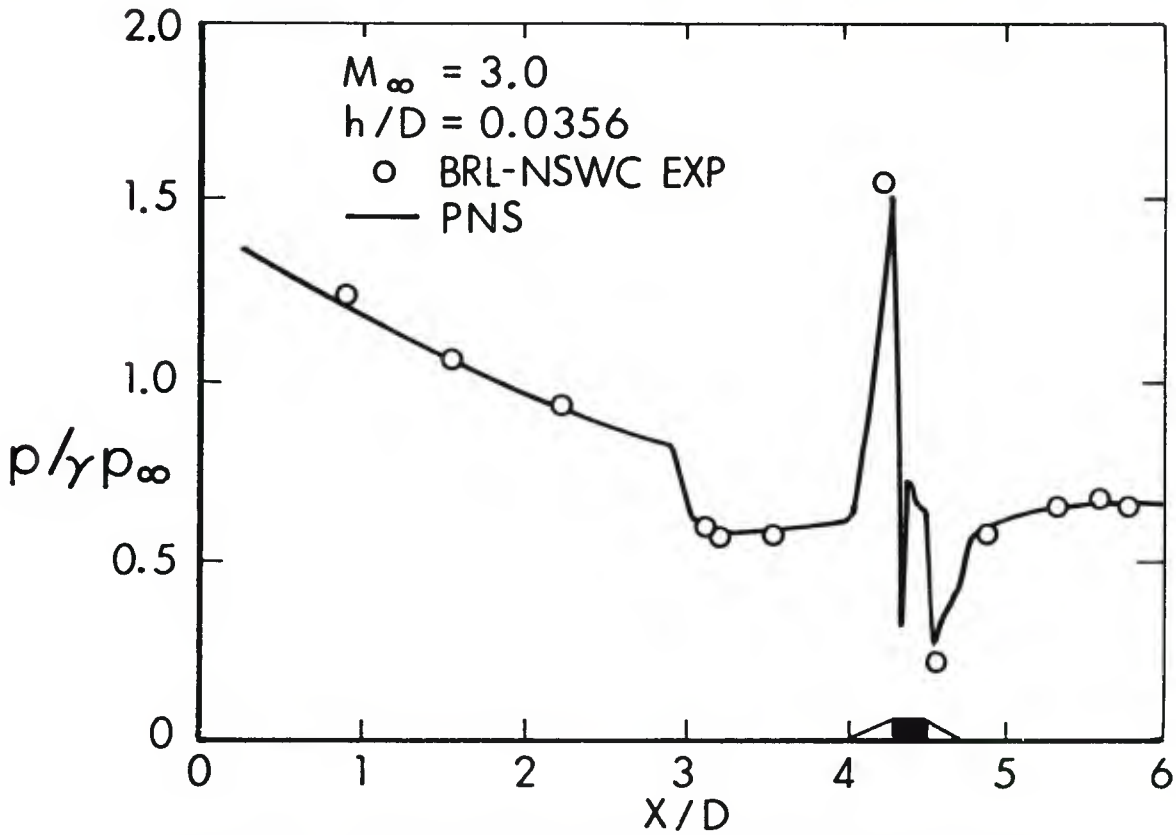

Figure 9. Pressure Distribution - Large Rotating Band

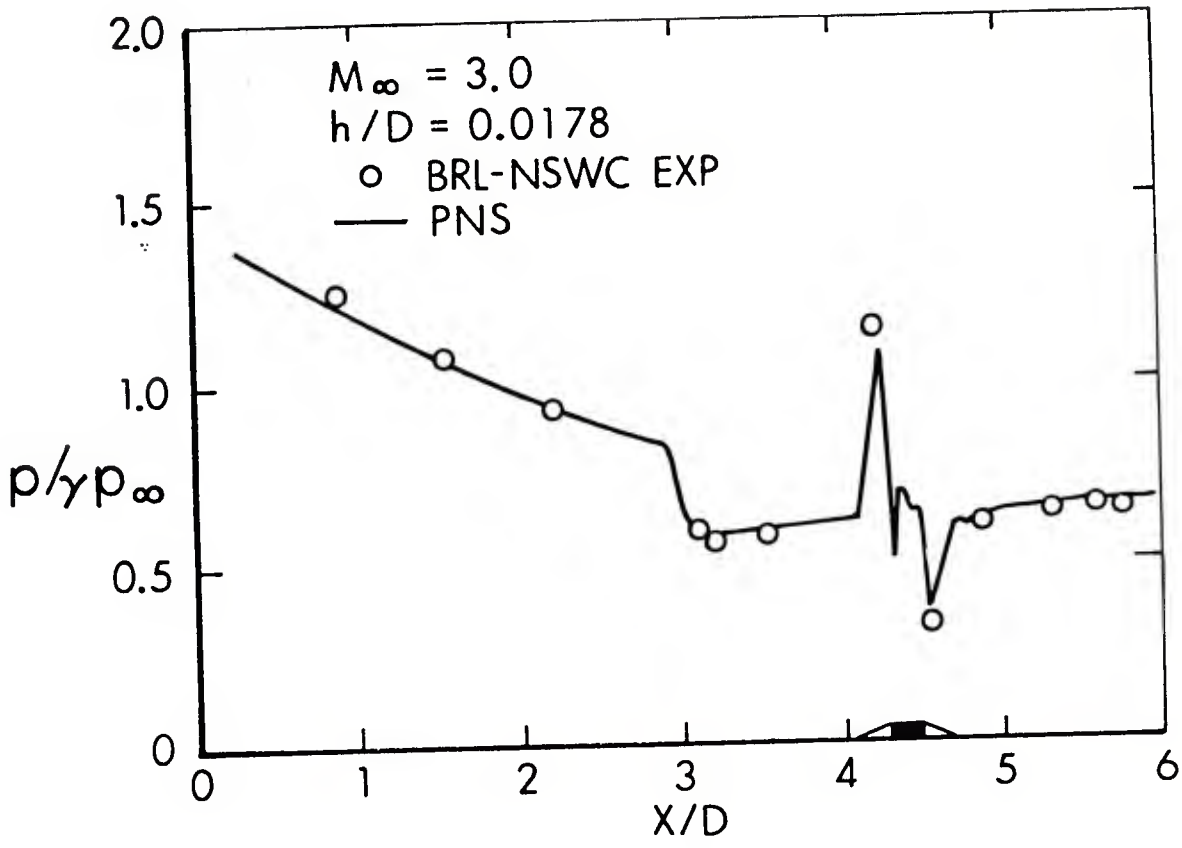

Figure 10. Pressure Distribution - Small Rotating Band

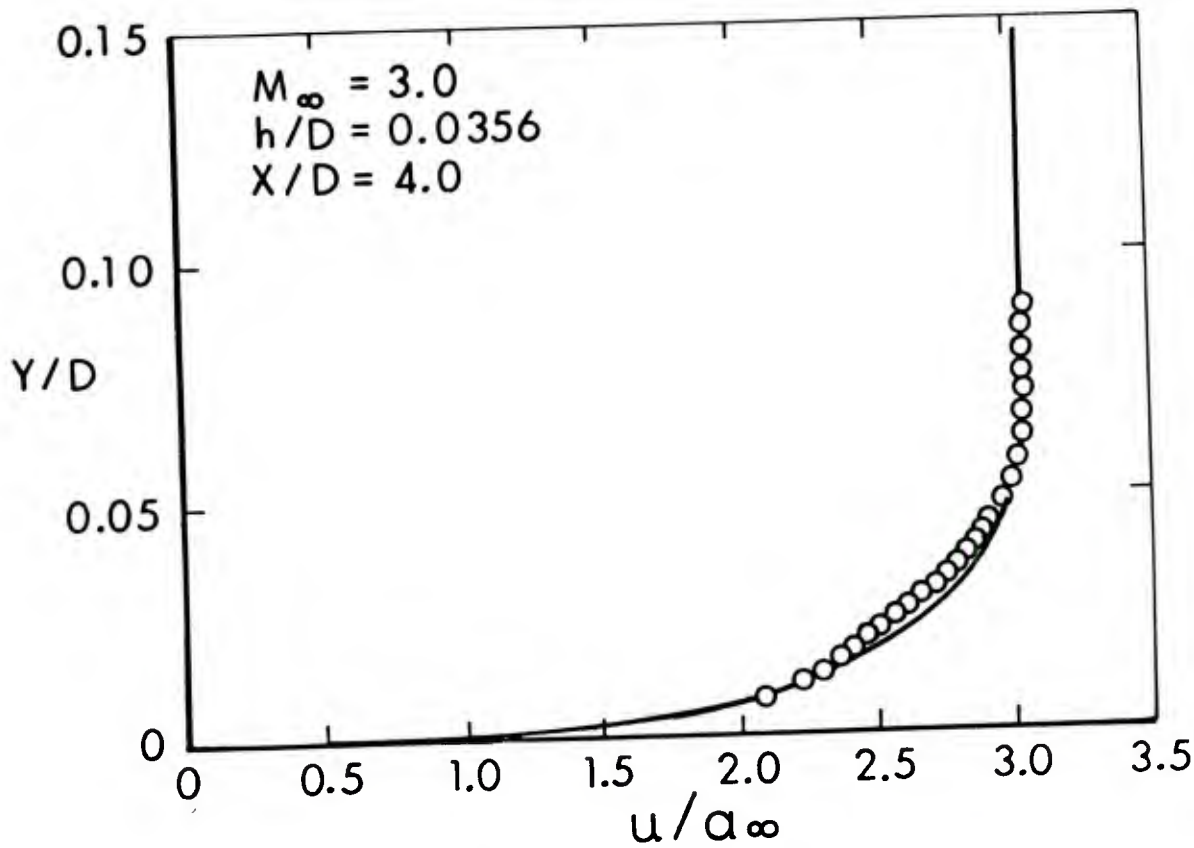

Figure 11. Velocity Profiles, h/D = 0.0356, M_∞ = 3.0

a. X/D = 4.0

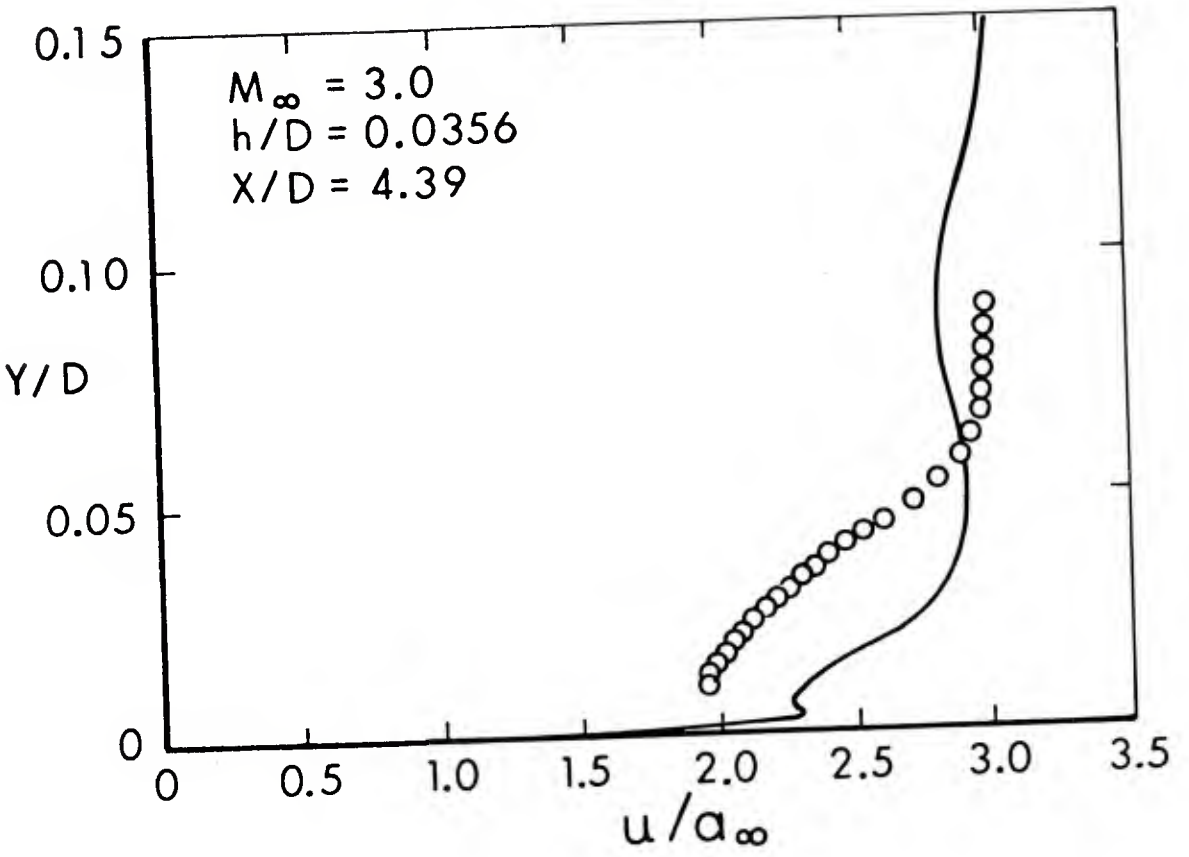

Figure 11. Continued

b. X/D = 4.39

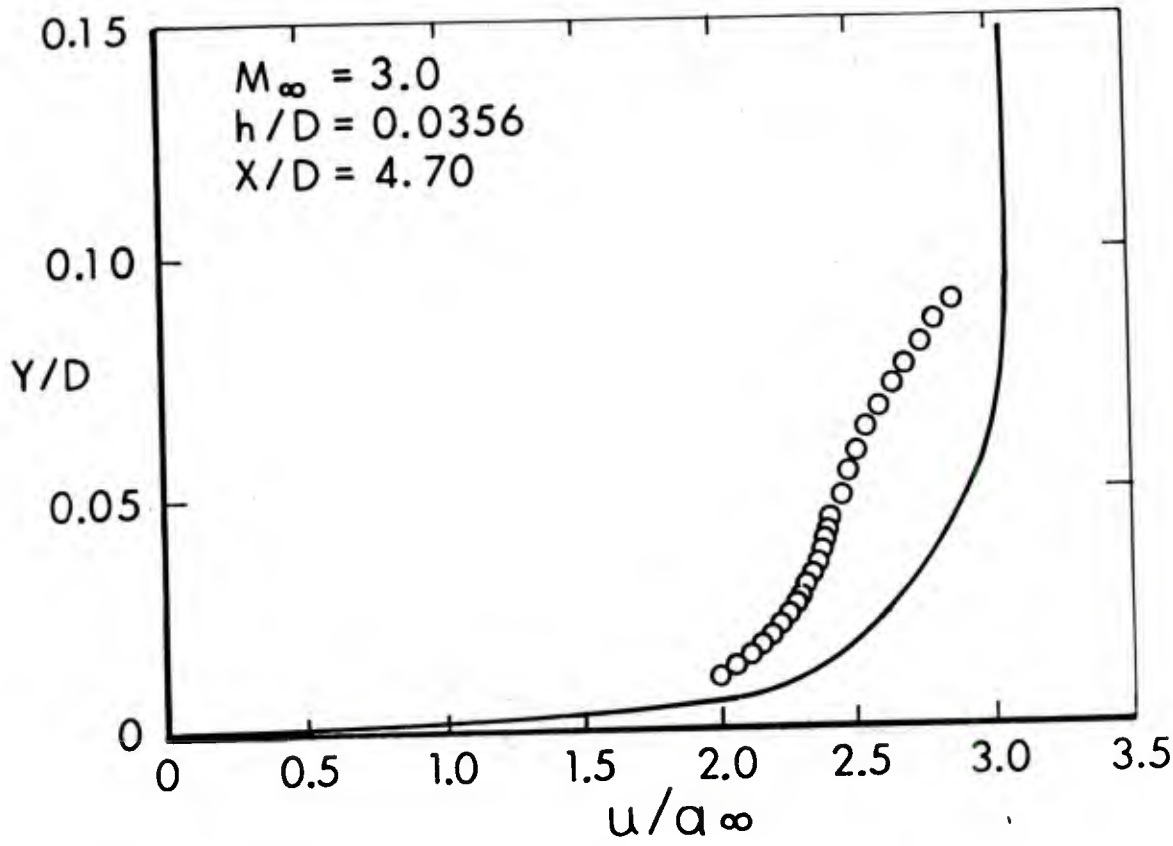

Figure 11. Continued

c. X/D = 4.70

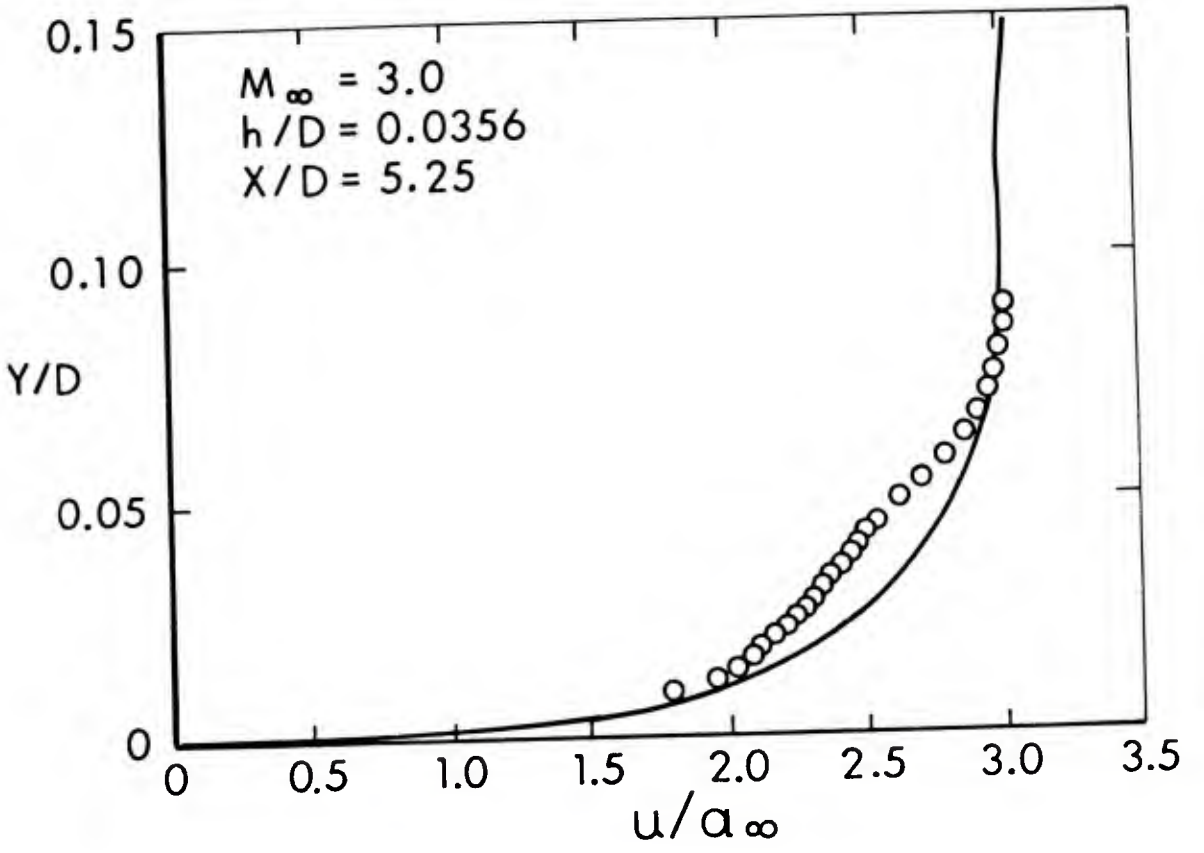

Figure 11. Continued

d. X/D = 5.25

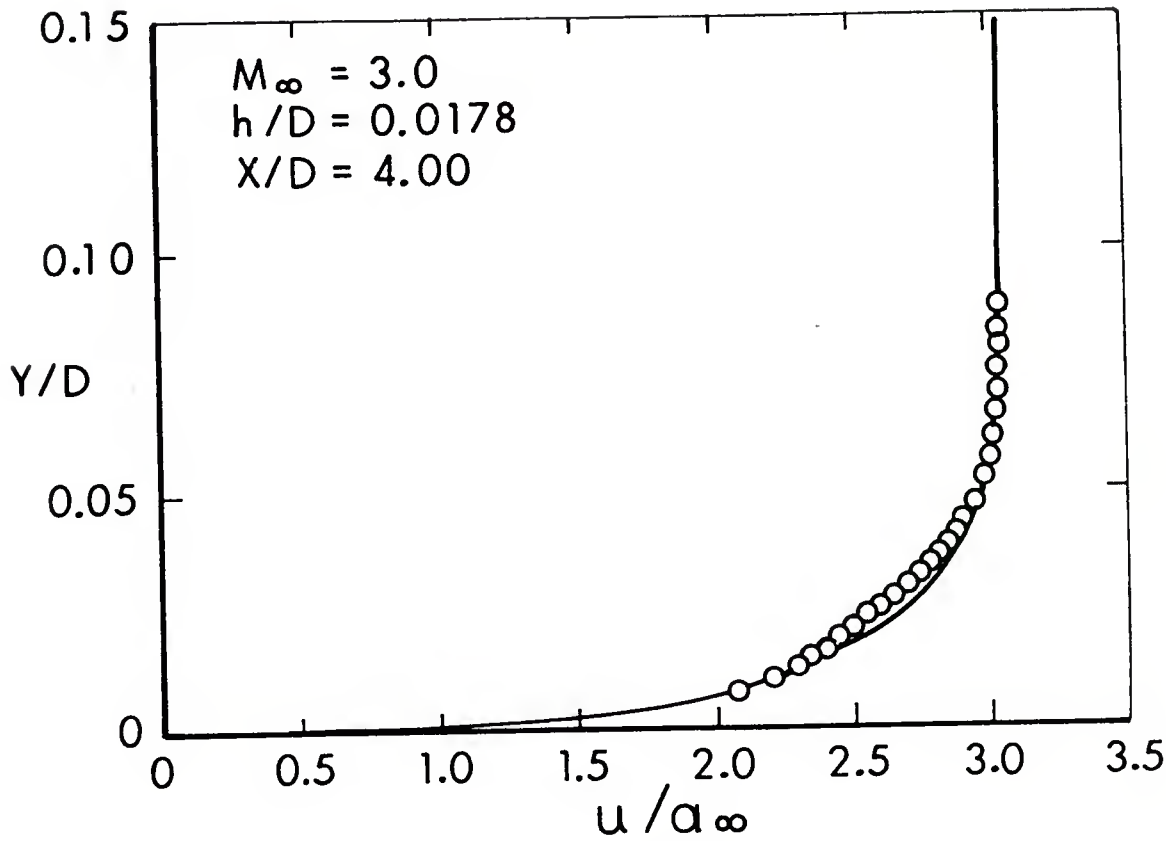

Figure 12. Velocity Profiles, h/D = 0.0178, M_∞ = 3.0

a. X/D = 4.0

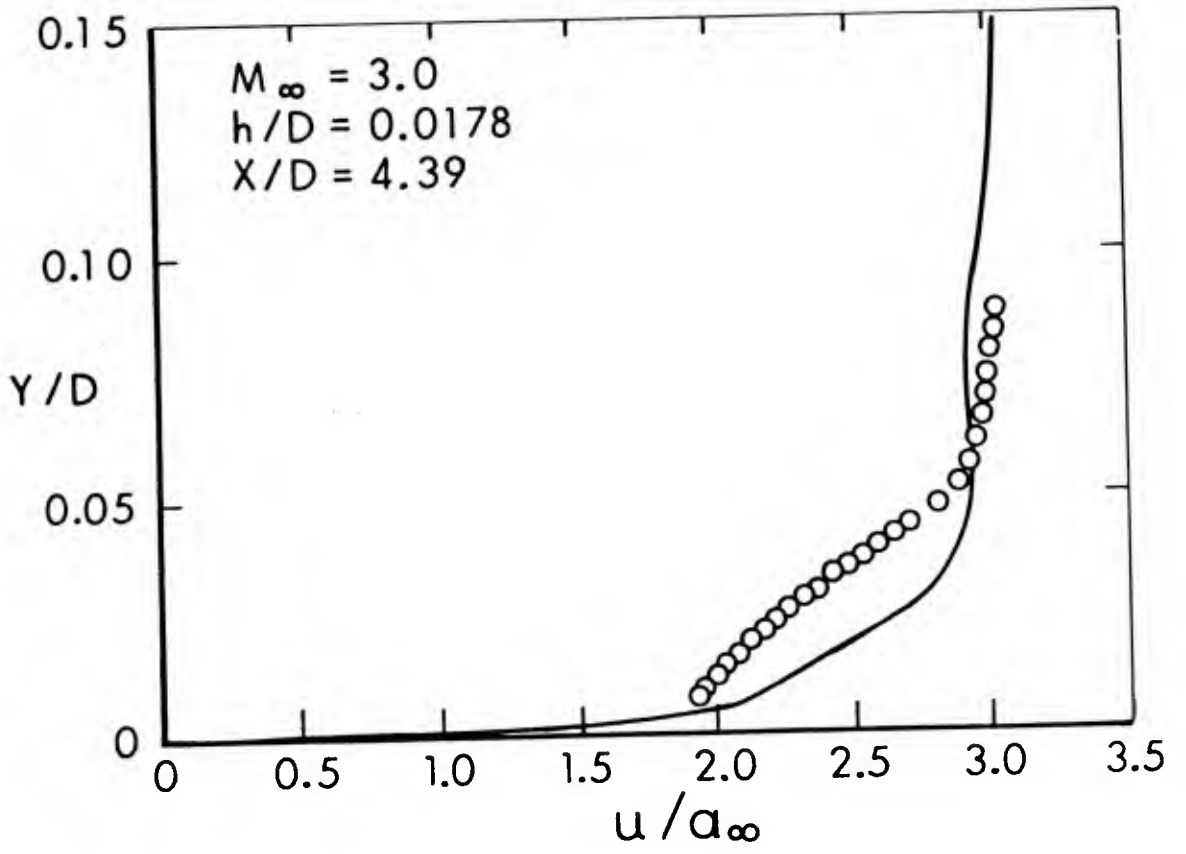

Figure 12. Continued

b. X/D = 4.39

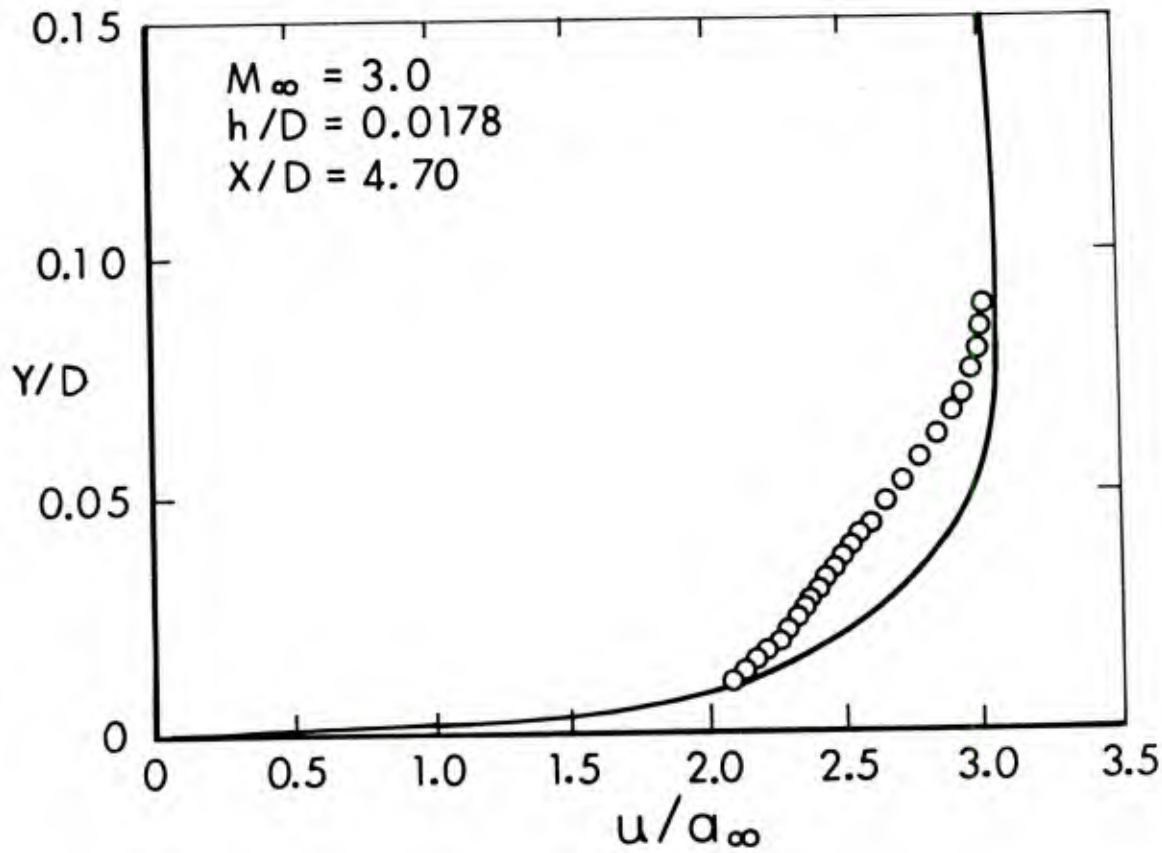

Figure 12. Continued

c. X/D = 4.70

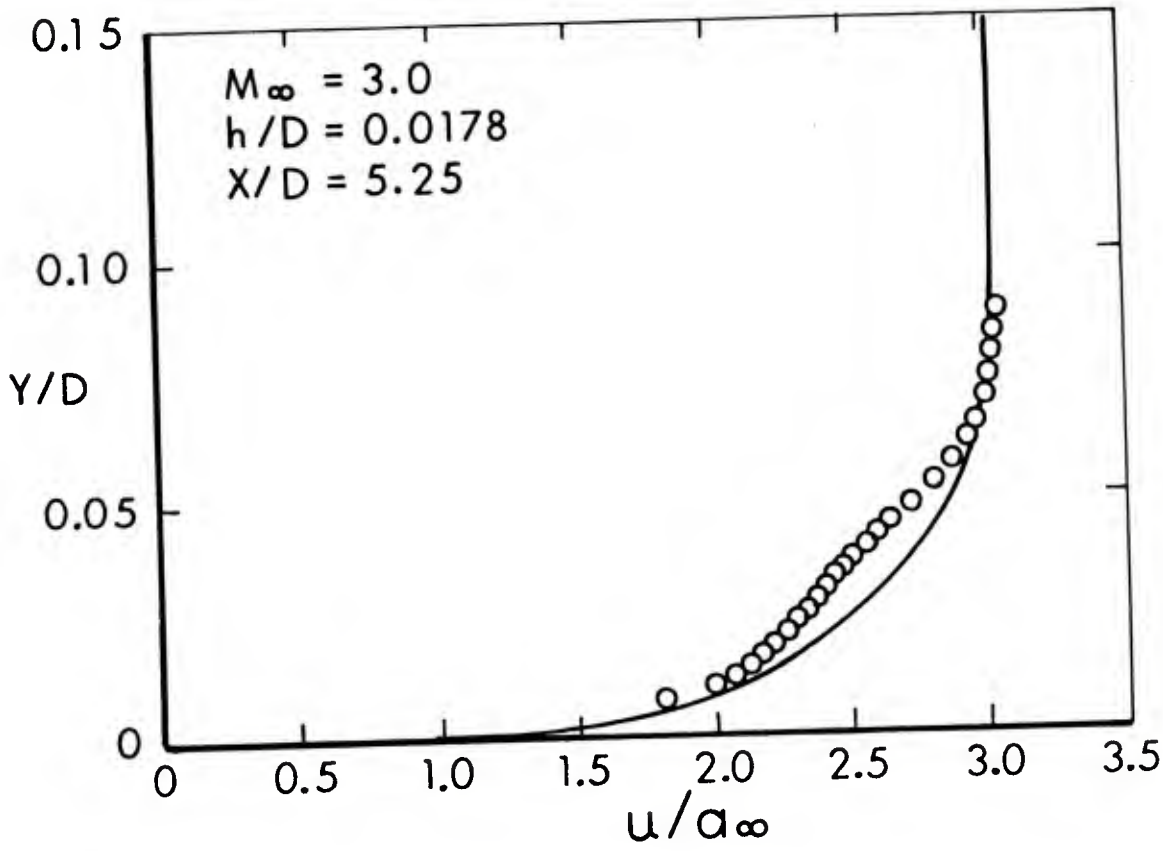

Figure 12. Continued

d. X/D = 5.25

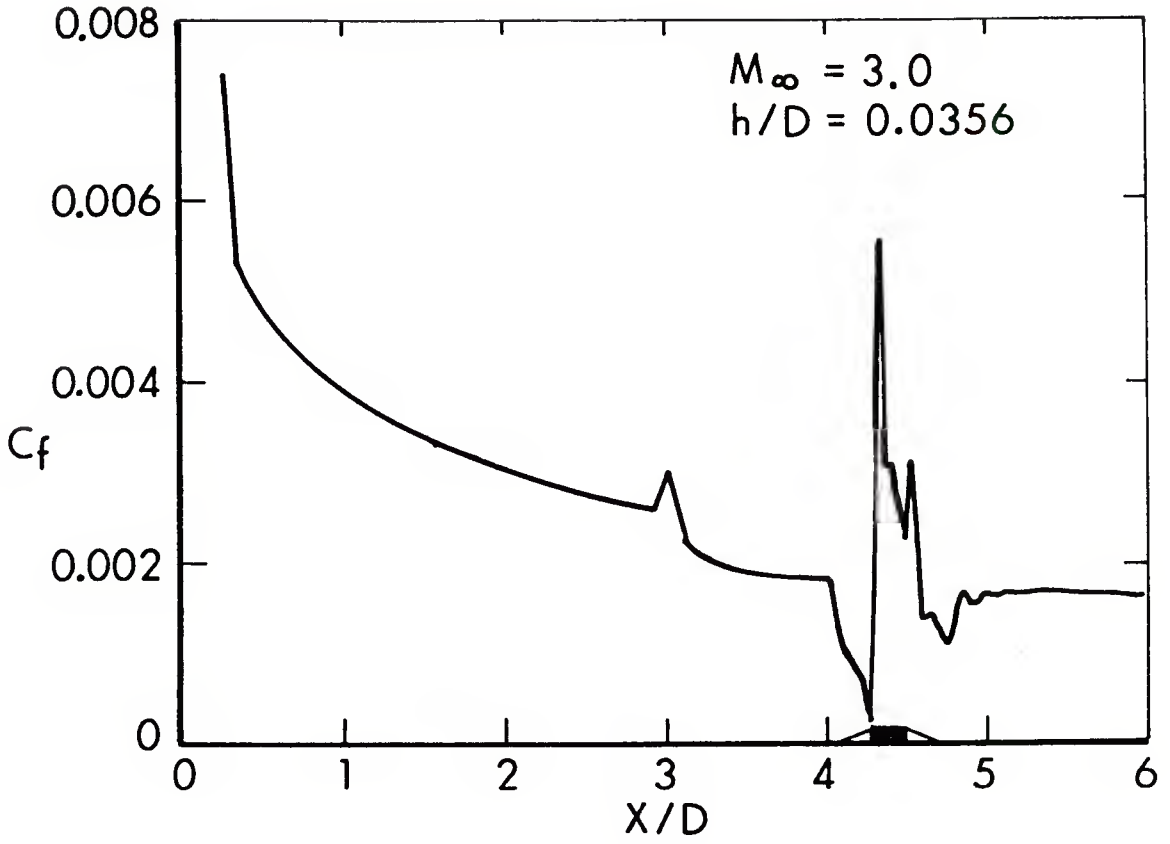

Figure 13. Skin Friction Coefficient Distribution, h/D = 0.0356, M_∞ = 3.0

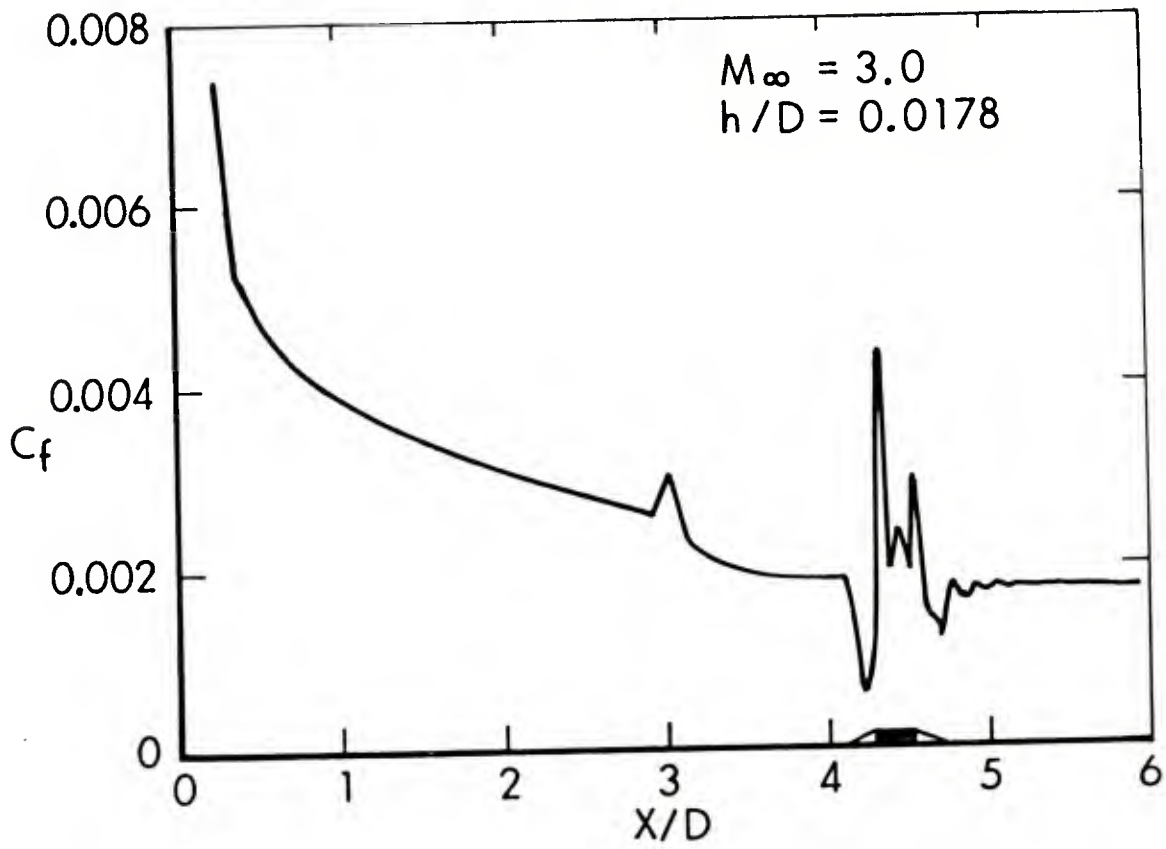

Figure 14. Skin Friction Coefficient Distribution, h/D = 0.0178, M_∞ = 3.0

REFERENCES

1. McCoy, R.L., "'MCDRAG' - A Computer Program for Estimating the Drag Coefficients of Projectiles," ARBRL-TR-02293, U.S. Army Ballistic Research Laboratory, ARRADCOM, February 1981 (AD A098110).

2. Moore, F.G., "Body Alone Aerodynamics of Guided and Unguided Projectiles at Subsonic, Transonic and Supersonic Mach Numbers," NWL Technical Report TR-2796, November 1972.

3. Moore, F.G., "A Study to Optimize the Aeroballistic Design of Naval Projectiles," NWL TR-2337, September 1969.

4. Charters, A.C., "Some Ballistic Contributions to Aerodynamics," Journal of Aeronautical Science, Vol. 14, No. 3, 1947, pp. 155-166.

5. Scott, W.E., "The Effect of Rotating Band Upon Some Aerodynamic Coefficients of the Seven Caliber Army-Navy Spinner Rocket at Mach 1.8," BRL-MR-1302, US Army Ballistic Research Laboratory, ARRADCOM, September 1960 (AD 246223).

6. Young, A.D., and Patterson, J.H., "Aircraft Excrescence Drag," AGARDograph No. 264, July 1981.

7. Sturek, W.B., and Schiff, L.B., "Numerical Simulation of Steady Supersonic Flow Over Spinning Bodies of Revolution," AIAA Journal, Vol. 20, No. 12, December 1982, pp. 1724-1731.

8. Chapman, D.R., Kuehn, D.M., and Larson, H.K., "Investigation of Separated Flows in Supersonic and Subsonic Streams with Emphasis on the Effect of Transition," NACA TN 3869, 1957.

9. Charwat, A.F., Roos, J.N., Dewey, C.F., and Hitz, J.A., "An Investigation of Separated Flows: Part I - The Pressure Field," Journal of the Aerospace Sciences, Vol. 28, No. 6, June 1961, pp. 457-470.

10. Yanta, W. and Gorney, J., NSWC/WOL unpublished wind tunnel data, private communication.

11. Reklis, R.P., and Sturek, W.B., "Surface Pressure Measurements on Slender Bodies at Angle of Attack in Supersonic Flow," ARBRL-MR-02876, U.S. Army Ballistic Research Laboratory, ARRADCOM, Aberdeen Proving Ground, MD 21005, November 1978 (AD A064097).

LIST OF SYMBOLS

$C_{D_{RB}}$	drag coefficient based on projectile cross-sectional area
C_D	drag coefficient based on frontal area of rotating band
C_f	skin friction coefficient
d_{RB}	rotating band diameter in calibers
D	projectile diameter
h	rotating band height
h^+	nondimensional rotating band height = $u_\tau h/\nu$
L	interaction length
M_∞	free-stream Mach number
p_∞	free-stream static pressure
p_o	free-stream total pressure
p_w	surface pressure
r	projectile radius
r_b	rotating band radius
T_o	free-stream total temperature
u_τ	shear velocity
x	axial distance from projectile nose
γ	ratio of specific heats
ν	kinematic viscosity

DISTRIBUTION LIST

No. of Copies	Organization
12	Administrator Defense Technical Info Center ATTN: DTIC-DDA Cameron Station Alexandria, VA 22314
1	Commander US Army Materiel Development and Readiness Command ATTN: DRCDMD-ST 5001 Eisenhower Avenue Alexandria, VA 22333
10	Commander US Army Armament Research and Development Command ATTN: DRDAR-TDC DRDAR-TSS DRDAR-LCA-F Mr. D. Mertz Mr. E. Falkowski Mr. A. Loeb Mr. R. Kline Mr. S. Kahn Mr. S. Wasserman Mr. H. Hudgins Dover, NJ 07801
1	Commander US Army Armament Materiel Readiness Command ATTN: DRSAR-LEP-L Rock Island, IL 61299
1	Director US Army Armament Research and Development Command Benet Weapons Laboratory ATTN: DRDAR-LCB-TL Watervliet, NY 12189
1	Commander US Army Aviation Research and Development Command ATTN: DRDAV-E 4300 Goodfellow Blvd. St. Louis, MO 63120
1	Director US Army Air Mobility Research and Development Laboratory Ames Research Center Moffett Field, CA 94035
1	Commander US Army Communications Rsch and Development Command ATTN: DRSEL-ATDD Fort Monmouth, NJ 07703
1	Commander US Army Electronics Research and Development Command Technical Support Activity ATTN: DELSD-L Fort Monmouth, NJ 07703
2	Commander US Army Missile Command ATTN: DRSMI-R DRSMI-RDK Mr. R. Deep Redstone Arsenal, AL 35898
1	Commander US Army Missile Command ATTN: DRSMI-YDL Redstone Arsenal, AL 35898
1	Commander US Army Tank Automotive Command ATTN: DRSTA-TSL Warren, MI 48090
1	Director US Army TRADOC Systems Analysis Activity ATTN: ATAA-SL White Sands Missile Range NM 88002
1	Commander US Army Research Office P. O. Box 12211 Research Triangle Park NC 27709

DISTRIBUTION LIST

No. of Copies	Organization
1	Commander US Naval Air Systems Command ATTN: AIR-604 Washington, D. C. 20360
2	Commander David W. Taylor Naval Ship Research and Development Center ATTN: Dr. S. de los Santos Mr. Stanley Gottlieb Bethesda, Maryland 20084
4	Commander US Naval Surface Weapons Center ATTN: Dr. T. Clare, Code DK20 Mr. P. Daniels Mr. D. A. Jones III Mr. L. Mason Dahlgren, VA 22448
4	Commander US Naval Surface Weapons Center ATTN: Code 312 Dr. W. Yanta Code R44 Dr. C. Hsieh Dr. T. Zien Dr. R. U. Jettmar Silver Spring, MD 20910
1	Commander US Naval Weapons Center ATTN: Code 3431, Tech Lib China Lake, CA 93555
1	Director NASA Langley Research Center ATTN: NS-185, Tech Lib Langley Station Hampton, VA 23365
2	Commandant US Army Infantry School ATTN: ATSH-CD-CSO-OR Fort Benning, GA 31905

No. of Copies	Organization
1	ACUREX Corporation/Aerotherm ATTN: Dr. M. J. Abbett 485 Clyde Avenue Mountain View, CA 94042
1	AVCO Corporation Research-Advanced Development Division 201 Lowell Street Wilmington, MA 01887
1	Nielsen Engineering & Research, Inc. ATTN: Dr. S. Stahara 510 Clyde Avenue Mountain View, CA 94043
2	Sandia Laboratories ATTN: Technical Staff, Dr. W.L. Oberkampf Aeroballistics Division 5631, H.R. Vaughn Albuquerque, NM 87115
1	Massachusetts Institute of Technology ATTN: Tech Library 77 Massachusetts Avenue Cambridge, MA 02139
1	University of Delaware Mechanical and Aerospace Engineering Department ATTN: Dr. J. E. Danberg Newark, DE 19711

Aberdeen Proving Ground

Dir, USAMSAA
ATTN: DRXSY-D
DRXSY-MP, H. Cohen

Cdr, USATECOM
ATTN: DRSTE-TO-F

Dir, USACSL, Bldg. E3516, EA
ATTN: DRDAR-CLB-PA
DRDAR-CLN
DRDAR-CLJ-L

USER EVALUATION OF REPORT

Please take a few minutes to answer the questions below; tear out this sheet, fold as indicated, staple or tape closed, and place in the mail. Your comments will provide us with information for improving future reports.

1. BRL Report Number _____

2. Does this report satisfy a need? (Comment on purpose, related project, or other area of interest for which report will be used.)

_____

_____

_____

3. How, specifically, is the report being used? (Information source, design data or procedure, management procedure, source of ideas, etc.) _____

_____

_____

4. Has the information in this report led to any quantitative savings as far as man-hours/contract dollars saved, operating costs avoided, efficiencies achieved, etc.? If so, please elaborate.

_____

_____

5. General Comments (Indicate what you think should be changed to make this report and future reports of this type more responsive to your needs, more usable, improve readability, etc.) _____

_____

_____

_____

6. If you would like to be contacted by the personnel who prepared this report to raise specific questions or discuss the topic, please fill in the following information.

Name: _____

Telephone Number: _____

Organization Address: _____

_____

_____